Available online at www.CivileJournal.org

Civil Engineering Journal

(E-ISSN: 2476-3055; ISSN: 2676-6957)

Vol. 11, No. 07, July, 2025

Analysis of Influence Factor of Soil-Structure Interaction Considered in Pile Analysis using Finite Element Analysis

Jin Kim [1], Jong-Young Lee [2], Da-Bi Lim [2], Jung-Geun Han [1, 2*]

[1] *Department of Intelligent Energy Industry, Chung-Ang University, Seoul, 06974, South Korea.*

[2] *Department of Civil Engineering, Chung-Ang University, Seoul, 06974, South Korea.*

Received 12 March 2025; Revised 21 June 2025; Accepted 25 June 2025; Published 01 July 2025

Abstract

This study evaluates two often-overlooked factors in pile analysis (passive earth pressure and the pile-soil contact method) and quantifies their combined influence on load–settlement response, shaft friction, and stress distribution. Conventional finite element analyses rarely consider both passive earth pressure and pile–soil slip simultaneously. This research quantifies the influence of these two factors on the load–settlement behavior, shaft friction, and stress transfer mechanisms of a single square pile. A laboratory model test was conducted using a 50 × 50 × 150 mm model pile embedded in loose sand with a relative density of 25%, and the same conditions were replicated using a 3D FEM model in ANSYS. The soil was modeled using the Mohr–Coulomb model, with parameters obtained from direct shear tests, and the pile was defined as a linear elastic material. The lateral boundaries were defined under two conditions: a general roller-type boundary and a new boundary condition incorporating depth-dependent passive earth pressure. Interface behavior was analyzed with both bonded and frictional contacts. The passive earth pressure boundary condition reduced post-yield settlement error from 22% to 6% and increased calculated shaft friction by 4%, resulting in a post-yield settlement curve that closely matched the experimental results. Bonded contact overestimated the bearing capacity by 17% and produced unrealistic stress concentrations, while Frictional contact accurately reproduced the observed slip surface and ultimate bearing capacity within a 3% margin of error. Parametric analysis revealed that the elastic modulus governed pre-yield stiffness, whereas the friction coefficient primarily influenced plastic deformation behavior. By combining the depth-dependent passive earth pressure boundary with experimentally calibrated frictional contact, this study successfully captured both lateral confinement effects and interface slip, which are typically analyzed separately. Consequently, the predictive accuracy for settlement and bearing capacity of friction piles in sandy soils was empirically improved.

Keywords: Soil-Structure Interaction (SSI); Finite Element Analysis (FEA); Model Test; Soil Parameter.

1. Introduction

Soil is a material characterized by significant heterogeneity and non-uniformity, and its physical and mechanical behavior varies with changes in time or environmental conditions. Due to these characteristics, accurately analyzing ground behavior is highly challenging. Among the various analytical methods employed in geotechnical engineering, the Finite Element Method (FEM) is widely used because it can comprehensively model soil–structure interaction (SSI) by incorporating various constitutive models [1-3]. Recently, there has been growing interest in SSI analysis that more precisely simulates the real behavior of materials, particularly in understanding how geotechnical structures such as piles and retaining walls respond to external loads [4-6].

In particular, piles transfer superstructure loads deep into the ground, developing their bearing capacity through shaft friction and end bearing [7-9]. In sandy soil, this load transfer mechanism induces horizontal displacement of the

* Corresponding author: jghan@cau.ac.kr

http://dx.doi.org/10.28991/CEJ-2025-011-07-04

surrounding soil, leading to the development of passive earth pressure, which is governed by factors such as the internal friction angle (ϕ), friction coefficient, and earth pressure state [10-12]. However, accurately reproducing these complex physical phenomena in numerical analysis requires comprehensive consideration of various parameters, including soil properties (c, ϕ, E, ν), boundary conditions (fixed or elastic), and the pile–soil contact method.

In most previous studies, to simplify the modeling process, the lateral boundaries of the soil domain were often treated as hinges or rollers [13-15], or elastic boundary conditions were applied using spring constants [16-18]. Some studies have compared the effects of general versus elastic boundary conditions on SSI [19-21], but most have focused only on self-weight stress and neglected lateral earth pressure. Although some research related to sheet piles [22-24] or seismic behavior of piles [25-27] has considered earth pressure partially, studies that incorporate depth-dependent passive earth pressure directly as boundary conditions to quantify actual lateral stresses around the pile remain rare. Consequently, the actual contribution of shaft friction and end bearing is often underestimated or overestimated, leading to discrepancies between numerical predictions and actual pile behavior.

Ohta and Nakata (2025) analyzed the behavior of pipe–soil interaction using 3D DEM, applying lateral force to a buried pipe and assigning periodic boundary conditions instead of conventional fixed ones. Their results indicated shear failure occurring on the passive side of the pipe and reported strong similarity to experimental outcomes [28]. Elsiragy et al. (2025) conducted experiments and numerical analyses (using Plaxis 3D) on laterally loaded piles, applying general boundary conditions but also incorporating self-weight and at-rest pressure coefficient (K_0) to more accurately simulate the effect of earth pressure [29]. Additionally, though there are prior studies addressing various boundary conditions in FEM (e.g., Mixed, Dirichlet, Neumann, Two-Point), their direct application in geotechnical soil models remains insufficient [30-32].

Bonded contact, a commonly used approach in FEM software, assumes perfect adhesion between the pile and soil with no slip or separation, often resulting in overestimation of pile resistance. In contrast, frictional contact better simulates actual slip and frictional behavior in sandy soils by considering parameters such as friction angle, contact stiffness, and surface roughness. However, there are relatively few studies where such parameters have been experimentally calibrated, and direct comparisons between Bonded and Frictional contacts are also limited. Moreover, studies that comprehensively analyze the interaction between boundary conditions (especially including lateral earth pressure) and contact methods in pile modeling using the Mohr-Coulomb model are even rarer.

To address these research gaps, this study proposes an alternative numerical modeling approach that incorporates "depth-dependent passive earth pressure" directly as a side boundary condition. It also systematically analyzes how numerical results change when applying both Bonded and Frictional contact approaches for SSI. Laboratory model tests were performed to measure the actual load–deformation behavior of a pile in sand, and the same conditions (soil properties, pile geometry, etc.) were used to construct a corresponding finite element model. Unlike conventional simple boundary conditions such as hinges or rollers, this study proposes a method that quantifies and applies lateral pressure by depth and then compares the effects of Bonded and Frictional contact separately.

In particular, the Frictional contact model incorporated internal friction angle and friction coefficients obtained from direct shear tests, ensuring the analysis is based on experimental data rather than assumed values. Furthermore, the numerical investigation considered not only cohesion (c) and internal friction angle (ϕ), but also self-weight stress, passive earth pressure distribution, boundary conditions, and contact methods. Their impact on pile settlement, moment distribution, and shaft friction was examined in a multi-faceted manner.

Finally, by comparing the numerical results with the laboratory experiments, the study evaluates how accurately the proposed model can reproduce the real behavior of the soil surrounding the pile when applying depth-dependent lateral earth pressure and Frictional contact. It also assesses how much analytical precision is improved compared to conventional boundary conditions and Bonded contact. This study highlights the often-overlooked role of lateral pressure modeling and the effectiveness of Frictional contact methods, ultimately providing a basis for improving accuracy and safety in future pile foundation design. The findings are expected to contribute to establishing clearer guidelines for selecting boundary conditions, contact modeling techniques, and soil properties in geotechnical analysis.

2. FEM of Geotechnical Engineering

To apply finite element analysis (Finite Element Method, FEM) in geotechnical engineering, it is essential to use a constitutive model that can appropriately simulate the behavior of soil, which is an inhomogeneous and nonlinear elasto-plastic material. Several models are commonly used for soil analysis, including the Linear Elastic model, Drucker-Prager model, Hardening Soil model, and Mohr-Coulomb model. The selection of a specific model depends on factors such as the analysis purpose, soil properties, and computational efficiency [33].

Unlike elastic materials (e.g., reinforced concrete and steel), soil exhibits nonlinear elasto-plastic behavior. Thus, a simplified linear analysis that does not account for this behavior can lead to significant discrepancies from actual soil response. This study focuses on analyzing pile behavior in sand and, after reviewing various nonlinear models, adopts the Mohr-Coulomb model as the constitutive model representing the elasto-plastic behavior of the soil.

2.1. Outline of the Mohr-Coulomb Model

The mohr-coulomb model is a linear elastic-perfectly plastic model. In the elastic region, the material behavior is governed by Hooke's Law, while in the plastic region, it follows the Mohr-Coulomb failure criterion. This model primarily uses cohesion (c) and internal friction angle (ϕ) as key parameters and is one of the most traditional and simple methods for simulating shear behavior in geotechnical engineering. In practical design and numerical analysis, values for c, φ, Young's modulus (E), and Poisson's ratio (ν) can be easily estimated through experiments or literature data, making the Mohr-Coulomb model widely used as an initial approach for numerical analysis [34, 35].

The yield function F({σ'},{k}) in the Mohr-Coulomb model represents the elasto-plastic properties of soil in their most general form. In FEA using the Mohr-Coulomb model, the analysis of the plastic region requires not only the yield function F, but also a separate plastic potential function P({σ'},{m}). In most cases, the plastic potential function P is set equal to the yield function F, allowing for the application of the associated flow theory.

$$F(\{\sigma'\},\{k\}) = \sigma_1' - \sigma_3' - 2c'cos\varphi' - (\sigma_1' + \sigma_3')sin\varphi' \quad (1)$$

The yield function F can be rewritten in terms of the stress invariants I, J, and θ as follows.

$$F(\{\sigma'\},\{k\}) = J_2 - \left(\frac{c'}{tan\varphi'} + I_1\right) \times \left(\frac{sin\varphi'}{\frac{cos\theta' - sin\theta' sin\varphi'}{\sqrt{3}}}\right) \quad (2)$$

where φ is Internal Friction Angle, I1 is First Stress Invariant, and J2 is Second Deviatoric Stress Invariant.

2.2. Non-Associated Flow Rule and Dilatancy

In geotechnical FEA, applying the associated flow rule, where the yield function *F* and the plastic potential function P are the same, can lead to infinite dilatancy, causing significant deviations from actual behavior. Therefore, to better simulate the real behavior of sand, the non-associated flow rule is applied, and the dilatancy angle (ψ) is set close to zero or to a small value to calibrate the model.

In this study, a non-associated flow rule is adopted for sand analysis, ensuring that the plastic potential function *P* has a shape similar to the overall yield surface. This adjustment prevents excessive overestimation of volumetric changes (dilatancy) after failure. Specifically, the plastic potential function P is defined to have a similar form to the yield function F, but with modified parameters such as the dilatancy angle, allowing for a more accurate reproduction of failure patterns observed in experiments. The revised plastic potential function P is given as follows [36]:

$$\mathrm{P}(\{\sigma'\},\{\mathrm{m}\}) = J_2 - \left[\left(\frac{c'}{\tan\varphi'} + I_1\right) \cdot \frac{\sin\varphi'}{\frac{\cos\theta' - \sin\theta'\sin\varphi'}{\sqrt{3}}}\right] = 0 \quad (3)$$

By rearranging the above plastic potential function, the final yield function is obtained as follows:

$$\frac{1}{3} I_1 sin\varphi' + \sqrt{J_2}\left(\frac{cos\theta' - sin\theta' sin\varphi'}{\sqrt{3}}\right) - cos\varphi' = 0 \quad (4)$$

2.3. Comparison with Other Models

To analyze soil nonlinearity, various soil constitutive models such as the Hardening Soil model, Cam-Clay model, Drucker-Prager model, and Mohr-Coulomb model are commonly employed. These constitutive models provide high accuracy by precisely simulating consolidation behavior, variable elastic modulus, and distinguishing between volumetric and shear plastic deformations. However, the application of these models requires numerous parameters. This increases computational complexity and consequently reduces analytical efficiency.

In contrast, this study utilizes cohesion (c) and internal friction angle (ϕ) values obtained from direct shear tests on sand. The Mohr-Coulomb model defines post-yield behavior using a linear relationship based solely on cohesion and internal friction angle, allowing for straightforward integration of these directly measured parameters without additional calibration procedures. On the other hand, employing models like Drucker-Prager or other constitutive models typically necessitates additional calibration procedures for parameter input, potentially increasing errors and uncertainties. Therefore, the Mohr-Coulomb model was selected as the constitutive model for this research.

The Mohr-Coulomb model reliably predicts pile behavior in sand using relatively simple and directly measurable parameters. Additionally, the Mohr-Coulomb parameters provided by ANSYS software are strain-independent, implying that the characteristics of the soil material do not vary with deformation and thus do not account for strain-softening or strain-hardening effects. Nonetheless, adjustments to residual internal friction angle (ϕre), residual cohesion (c_{re}), and dilatancy angle (ψ), along with the application of non-associated flow rules, were implemented to accurately replicate the post-yield soil behavior closely resembling actual sand.

3. Laboratory Model Test

This study conducted a laboratory model test to closely examine pile behavior in sand and to identify influencing factors that should be considered in finite element analysis (FEM) [37, 38]. This chapter provides a brief description of the characteristics of the sand and model pile used in the experiment, as well as the fabrication of the model ground and the experimental procedures. The data obtained from the experiment were used to compare and analyze numerical simulations, helping to define the necessary parameters and boundary conditions for SSI analysis [39-41].

The maximum dry unit weight of the sand used in the experiment was 1.571 g/cm³, while the minimum dry unit weight was 1.388 g/cm³. The relative density (Dr) was set at 25%, replicating the conditions of naturally loose sand. The most critical parameters in the Mohr-Coulomb model are the internal friction angle (ϕ) and cohesion (c), which were determined through direct shear tests prior to the experiment. The test results showed that the internal friction angle of the sand was 30.8°, and the cohesion was 0.0054 N. The model soil box was constructed using a rigid frame with dimensions of 330 mm (width) × 330 mm (length) × 350 mm (height). The sand was placed and compacted in layers to ensure a uniform relative density. The box was designed with sufficient thickness and rigidity to minimize distortions in the lateral earth pressure and to maintain realistic soil conditions around the pile. The model pile was made of acrylic material with a cross-section of 50 mm × 50 mm and a length of 150 mm. However, due to the smooth surface of acrylic, it was difficult to simulate the frictional behavior between concrete and sand. To address this, crushed concrete powder was applied to the surface of the model pile to better simulate the actual pile-soil contact behavior. This surface treatment was intended to realistically capture shaft friction, which plays a crucial role in pile-soil interaction and soil deformation observations.

The experimental procedure was as follows. First, the sand was placed and compacted in layers while carefully maintaining a relative density of 25%. After installing the model pile, a step load was applied to the pile head, and at each stage, the pile head displacement was measured using an LVDT. Based on these measurements, load-displacement curves were plotted. Special attention was given to observing how shaft friction develops in sand and assessing the influence of Mohr-Coulomb model parameters by carefully monitoring pile displacement at each loading step [42, 43]. The load-displacement curve from this experiment serves as a reference for validating FEA models. This study systematically examines overlooked factors in SSI analysis, including boundary conditions and contact methods. By comparing experimental data with numerical results using different boundary conditions, contact methods, and Mohr-Coulomb parameters, it aims to refine numerical modeling for more accurate pile behavior simulation.

4. FEM Modeling

In this study, ANSYS (2021), a 3D finite element analysis (FEA) program, was used to analyze the SSI. This software is based on the finite element method (FEM) and offers various simulation capabilities, including linear and nonlinear analysis, dynamic analysis. Before the modeling process, the pile was defined as an elastic model with the material properties of concrete, while the soil was modeled using the Mohr-Coulomb model. In ANSYS, the Mohr-Coulomb model requires input parameters such as Young's modulus (E), Poisson's ratio (ν), internal friction angle (ϕ), cohesion (c), as well as dilatancy angle (ψ), residual cohesion (c_{re}), and residual internal friction angle (ϕ_{re}). Based on the direct shear test results, the internal friction angle and cohesion were set, while the dilatancy angle was set to zero to account for the non-associated flow rule. Considering that the sand used in the physical model test was a non-cohesive soil, the residual cohesion was also assumed to be zero. The material properties used for the pile and soil entities are summarized in Table 1.

Table 1. Material property

	ϕ (°)	c (N)	E (MPa)	ν	D_r (%)	γ (kg/m^3)	ψ (°)	ϕ_{re} (°)	c_{re} (N)
Sand	30.8°	0.0054	3~7	0.3	25%	1,430	0	23	0
Pile	-	-	30,000	0.15	-	2,300	-	-	0

The numerical analysis model was constructed in a three-dimensional space, where the sand inside the soil box and the pile were modeled as separate volumes. The model and mesh configuration are presented in Figure 1. The soil domain was defined with dimensions of 330 × 330 × 50 mm, matching the size of the soil box used in the laboratory test, and the pile was modeled as a 50 × 50 × 150 mm volume. The pile entity, assumed to exhibit elastic behavior, was discretized using a minimal number of elements, while the soil entity was meshed with more refinement. Approximately 11,000 elements were employed for the soil model. Various mesh sizes were examined during the finite element analysis (FEA), and the mesh that most accurately replicated the experimental behavior was selected for the final model. The pile was modeled as a linear elastic material, whereas the Mohr-Coulomb constitutive model was applied to the soil domain.

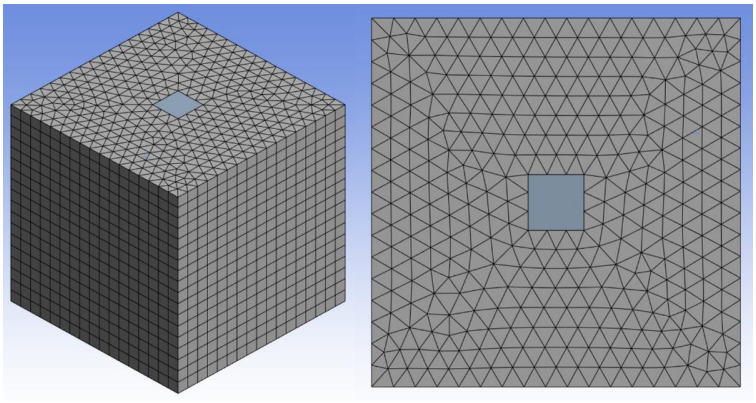

Figure 1. Model and mesh configuration

A fixed boundary condition was applied to the bottom of the soil model, restricting both displacements and rotations. Although previous studies have often simplified the side boundaries of the soil box using hinge or roller conditions, this study considered the potential development of passive earth pressure along the sidewalls. Accordingly, an alternative analysis was conducted in which earth pressure was applied to represent a more realistic boundary condition (Section 5.1.1). Contact between the pile and the surrounding soil was defined to simulate shaft friction and sliding at the interface. In ANSYS, contact interactions are implemented using CONTA and TARGE elements [44-46]. To account for the relative sliding that occurs during pile movement in sand, the frictional contact method was adopted in this study. For comparative and validation purposes, an additional analysis was also performed using the bonded contact method, where the pile and soil remain fully attached. This comparison allowed for an evaluation of the influence of contact methods on SSI analysis (Section 5.1.2).

The analysis procedure began by defining the initial contact state between the pile and the soil, followed by an initial equilibrium analysis considering self-weight and initial earth pressure. A nonlinear static analysis based on the Newton–Raphson iterative algorithm was performed, wherein each load step proceeded only after the residual force converged within a predefined tolerance. To more accurately capture the separation and sliding behavior at the pile-soil interface, the Augmented Lagrange contact formulation was employed. Subsequently, vertical loads up to 3500 N were incrementally applied to the pile head, and nonlinear soil behavior was analyzed under each load step. At every stage, critical responses such as plastic yielding, contact separation or slip, displacement, and stress distribution were closely monitored. Ultimately, load-displacement curves and soil deformation patterns surrounding the pile were obtained.

In this study, numerous simulations were conducted by adjusting influencing factors and parameters to achieve load–settlement behavior consistent with the experimental results. Density and internal friction angle values were directly adopted from laboratory tests, whereas the elastic modulus and friction coefficient were calibrated based on their agreement with the experimental data. Figure 2 compares the load–settlement curves obtained from laboratory testing and ANSYS simulations. While slight discrepancies were observed in the elastic range around 1,500–1,800 N, the plastic behavior beyond yielding closely matched the experimental results. These findings confirm that the bearing capacity of the pile, particularly in the ultimate load range, was accurately replicated through the numerical model. The overall procedure of the FEA is presented as a flowchart in Figure 3.

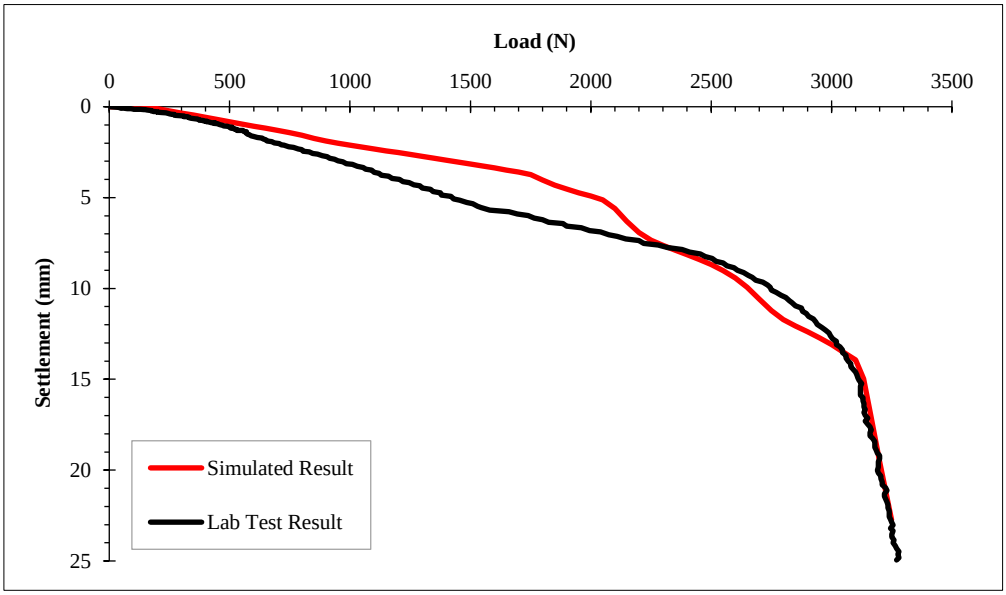

Figure 2. Load-Settlement Curves from Lab Test and FEM Simulation

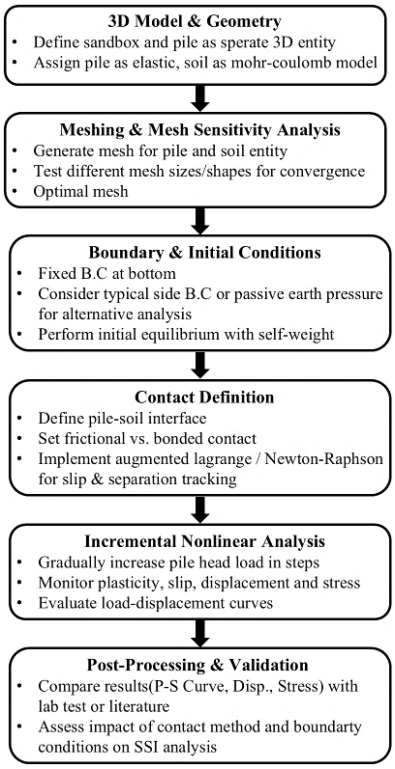

Figure 3. Schematic Illustration of the Pile–Soil Finite Element Analysis Process

5. Result of FEA

5.1. Influence Factor

5.1.1. Boundary condition

In pile numerical analysis, boundary conditions are often simply constrained using a hinge or roller, allowing for rotation. However, in sand, it is well known from static equations that shaft friction is directly influenced by earth pressure [47]:

$$f_S = K \cdot \sigma \cdot tan\delta \tag{5}$$

where f_S is Shaft friction, K is Coefficient of earth pressure, and δ is Friction angle between soil and pile.

Earth pressure is determined by the unit weight and internal friction angle of the soil. In the case of a pile installed in sand, when a force is applied to the pile head, it inevitably displaces the surrounding soil laterally, generating passive earth pressure. This leads to shaft friction that exceeds the typical friction force between the pile and sand.

Therefore, this study compared two lateral boundary conditions: one using a simple roller constraint and the other applying a depth-dependent passive earth pressure function (Soil Pressure B.C.), as shown in Figure 4. The Soil Pressure B.C. was implemented by applying passive earth pressure, calculated based on soil unit weight and internal friction angle, in an incremental form with depth.

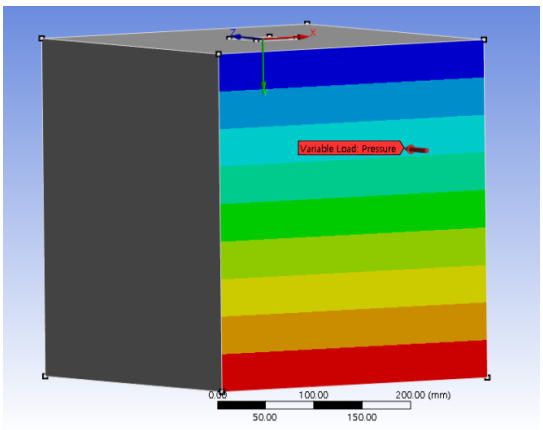

Figure 4. Soil Pressure Boundary Condition

According to the results shown in Figure 5, both boundary conditions exhibited similar bearing capacity, but differences occurred in the settlement behavior within the plastic region. Notably, above 3,100N, the boundary condition considering earth pressure more accurately reproduced the settlement behavior observed in the experiment. Although plastic region behavior differed between the two methods, the overall bearing capacity remained almost the same. However, differences were observed in the distribution of bearing capacity. Pile bearing capacity consists of a combination of tip resistance and skin friction, with the load distribution varying depending on soil conditions. Since the soil used in this study was sand, the pile behaved as a friction pile. In the numerical analysis, shaft friction in the Soil Pressure B.C. case was evaluated at approximately 0.918 MPa, which was about 4% higher than in the Hinge B.C. case (0.873 MPa).

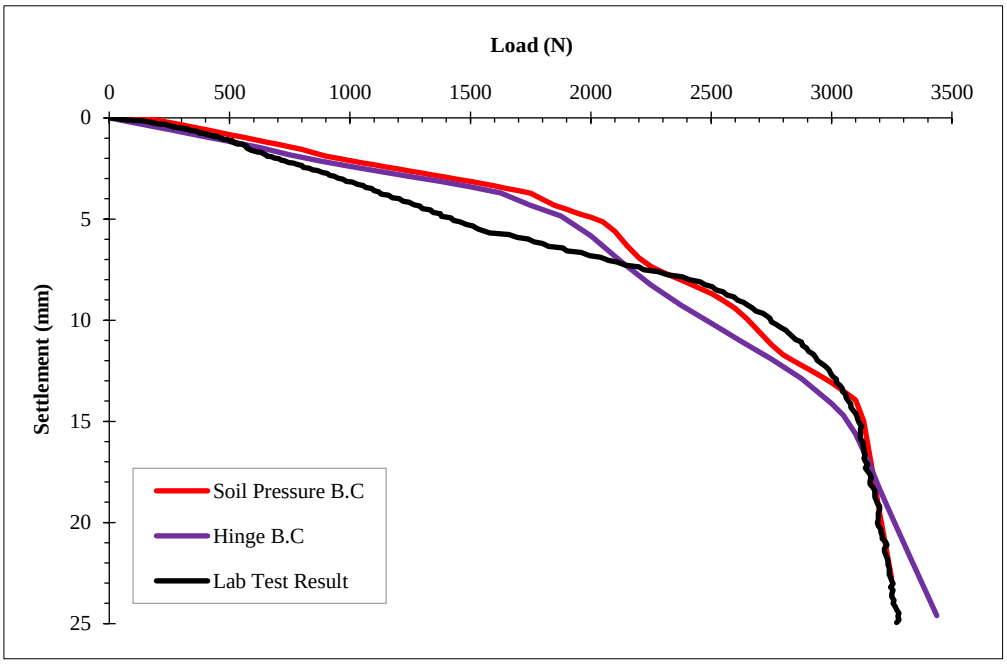

Figure 5. Load-Settlement Curves under Boundary Conditions

Figure 6 shows the stress distribution at the final load step. Overall, shaft friction was more actively developed in the soil pressure B.C case compared to roller B.C. Notably, the stress observed near the pile head at the ground surface was 0.023 MPa for soil pressure B.C. and 0.011 MPa for roller B.C, indicating a difference of more than twice. The higher stress at the pile head near the surface suggests that passive earth pressure was effectively activated.

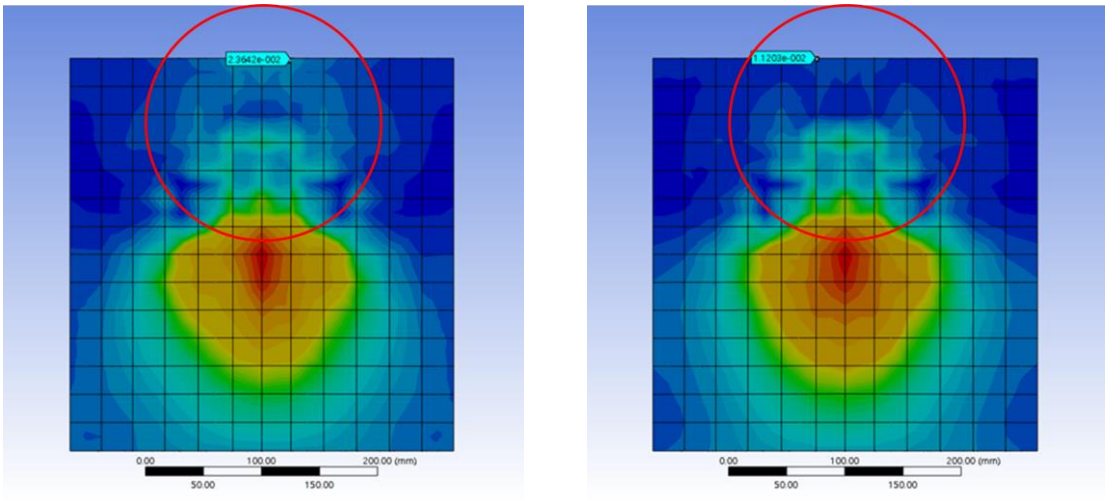

(a) Soil Pressure Boundary Condition (b) Roller Boundary Condition

Figure 6. Stress Distribution under Boundary Conditions

Figure 7 shows the stress distribution at the final load step. Overall, shaft friction was more actively developed in the soil pressure B.C case compared to roller B.C. Notably, the stress observed near the pile head at the ground surface was 0.023 MPa for soil pressure B.C. and 0.011 MPa for roller B.C, indicating a difference of more than twice. The higher stress at the pile head near the surface suggests that passive earth pressure was effectively activated. Differences were also observed in the settlement pattern. Figure 8 illustrates the vertical settlement at the final load step, showing that soil pressure B.C (Figure 7-a). had a wider influence on the surrounding soil compared to roller B.C (Figure 7-b). These results suggest that while boundary condition differences may not significantly affect overall bearing capacity, considering passive earth pressure leads to a more accurate representation of friction pile behavior in sand. Thus, soil pressure B.C. should be considered more advantageous for realistic geotechnical modelling.

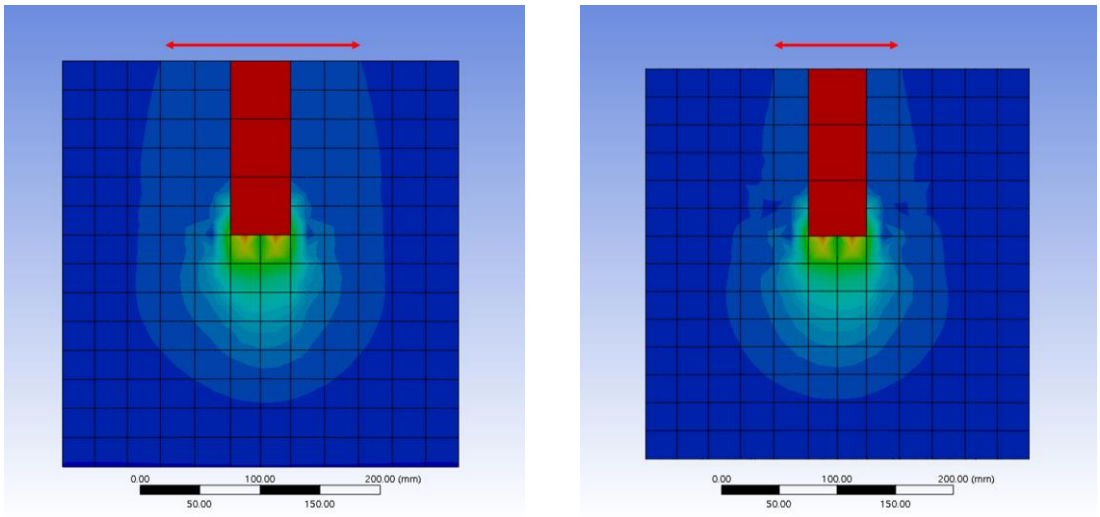

(a) Soil Pressure Boundary Condition (b) Hinge Boundary Condition

Figure 7. Difference in Settlement under Boundary Conditions

2.1.2. Contact Method

In numerical analysis, various methods exist for handling contact between different elements. Depending on the method, the analysis can be classified as linear or nonlinear, and the consideration of sliding between nodes also varies. In this study, bonded contact was applied to the pile tip, while the shaft-soil interface was analyzed using both bonded and frictional contact to compare the effects of different contact methods on the results. In previous ANSYS-based pile analyses, researchers commonly introduced a 1–3 mm gap between the pile shaft and soil and applied bonded contact. However, in this study, two models were compared and analyzed: one using frictional contact without a gap, and another using bonded contact with a gap. For the contact analysis algorithm, multiple methods were tested, and those with the highest agreement between numerical results and experimental data (ex: Normal Lagrange Method, Augmented Lagrange Method) were selected. The pile tip, connected via bonded contact, was constrained in the vertical direction, while the shaft was analyzed using the augmented lagrange method, allowing for vertical movement to simulate frictional behavior.

As shown in Figure 8-a, the bonded contact model exhibited higher bearing capacity in the load-settlement curve compared to the experimental results. This is because the pile and soil were fully bonded, preventing any relative sliding, which led to an overestimation of stiffness. This effect is clearly reflected in the stress distribution (Figure 8-b) and settlement pattern (Figure 8-c) obtained from the bonded contact analysis, where excessive stress was observed around the pile shaft. Even when a small gap was introduced between the pile and soil, the Bonded nodes still induced greater settlement in the surrounding soil, resulting in an artificially high shaft friction value. In contrast, the frictional contact method successfully simulated the gradual reduction in shaft friction and the occurrence of sliding as the pile entered the plastic region. As a result, the load-settlement curve closely matched the experimental data, highlighting that material parameters such as elastic modulus and friction coefficient can have varying effects depending on the contact method. Ultimately, it can be concluded that frictional contact provides a more accurate modeling approach for simulating pile behavior in sand, as it better represents the actual experimental response.

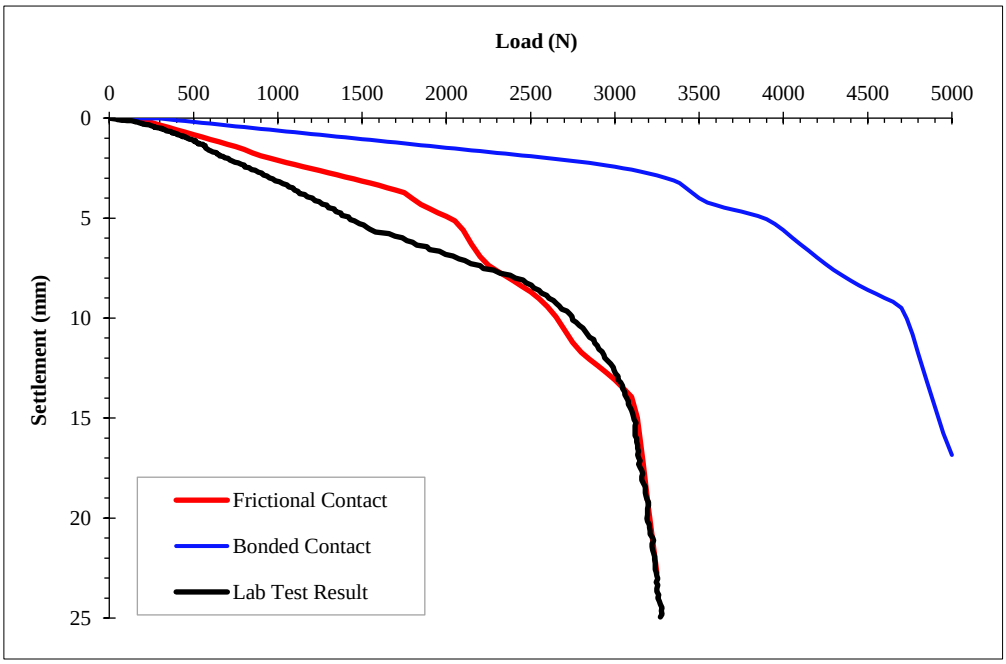

(a) Load-Settlement Curves under Different Contact Methods

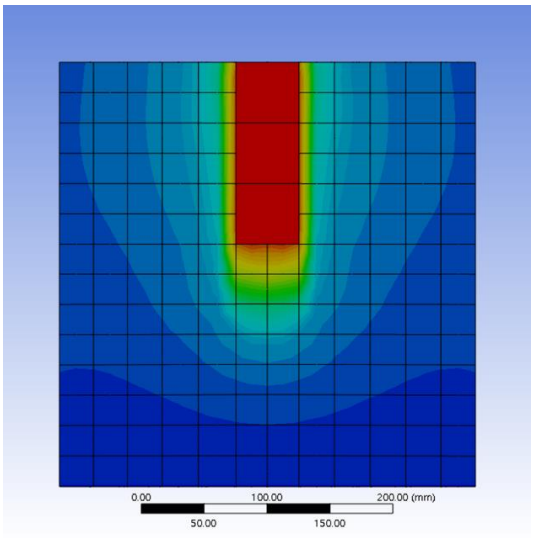

(b) Settlement of Bonded Contact

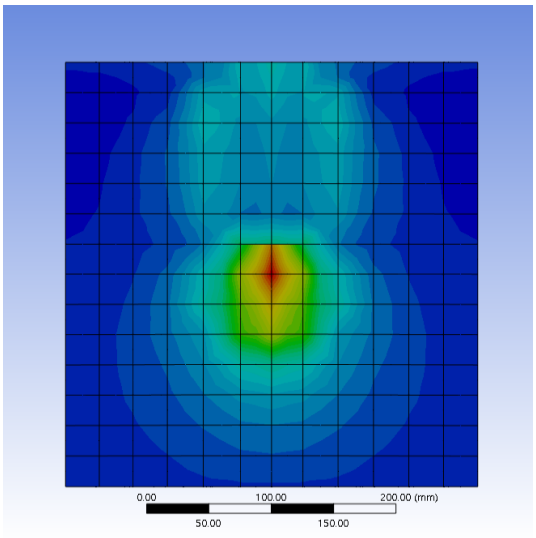

(c) Stress of Bonded Contact

Figure 8. Results of Bonded Contact FEM Analysis

5.2. Parameter

5.2.1. Elastic Modulus

The elastic modulus is a key parameter governing the linear behavior before yield, determining the stiffness of the soil. According to empirical estimates in the literature [47], loose sand with a relatively low density (Dr) and an internal friction angle of approximately 33° typically has an elastic modulus of 10,000 kPa or lower. However, as soil itself is not elastic, the elastic modulus cannot be directly measured; thus, empirical estimates from the literature are commonly employed. Therefore, this study examined variations in load-settlement behavior by applying different elastic modulus values (3, 5, and 7 MPa), while all other conditions remained constant. As shown in Figure 9, a higher elastic modulus resulted in reduced initial settlement and altered settlement patterns after yielding. Lower elastic modulus values (3–5 MPa) exhibited linear behavior similar to experimental results in the pre-yield region, but a value of 7 MPa was found to more accurately replicate the post-yield plastic behavior. This finding suggests that accurately predicting settlement near the ultimate bearing capacity of a pile requires considering not only the linear region but also the characteristics of plastic deformation in the post-yield region when determining the elastic modulus.

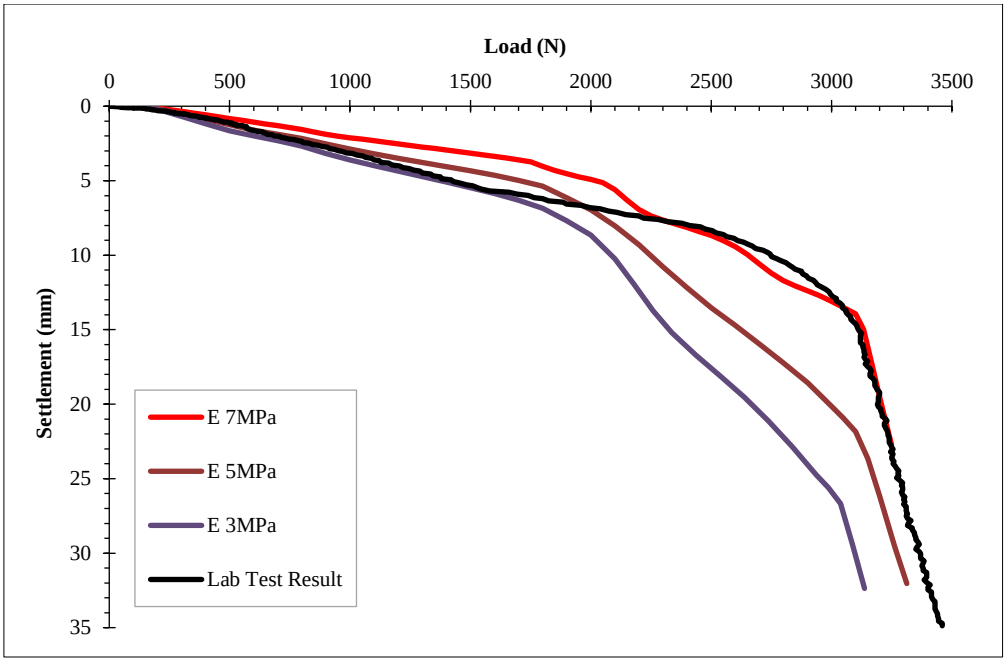

Figure 9. Load-Settlement Curves for Various Elastic Modulus

5.2.2. Frictional Coefficient

In this study, instead of using the gap + bonded contact method, a nonlinear frictional contact method was adopted to address soil-structure interaction (SSI). When using the frictional contact method in ANSYS, the friction coefficient parameter is required to simulate the interaction between materials. Although the model pile used in the laboratory test was made of acrylic, it was coated with concrete powder to replicate the surface roughness of real concrete. According to existing literature, the friction coefficient between concrete and sand typically ranges from 0.3 to 0.4 [48, 49].

In the FEA, three friction coefficient values were tested: 0.3 (in line with literature), and two higher values 0.5 and 0.7. Figure 10 shows that variations in the friction coefficient had little impact on both the linear and plastic regions of the load-settlement curve. However, the curve that best matched the experimental results was obtained using a friction coefficient of 0.5, which is slightly higher than the values reported in the literature. This suggests that, as sand has nearly no cohesion, the friction along the pile surface is the primary contributor to shaft resistance. Therefore, to more accurately reflect the surface roughness conditions in the experiment, using a slightly higher friction coefficient than literature values can help reduce modeling errors.

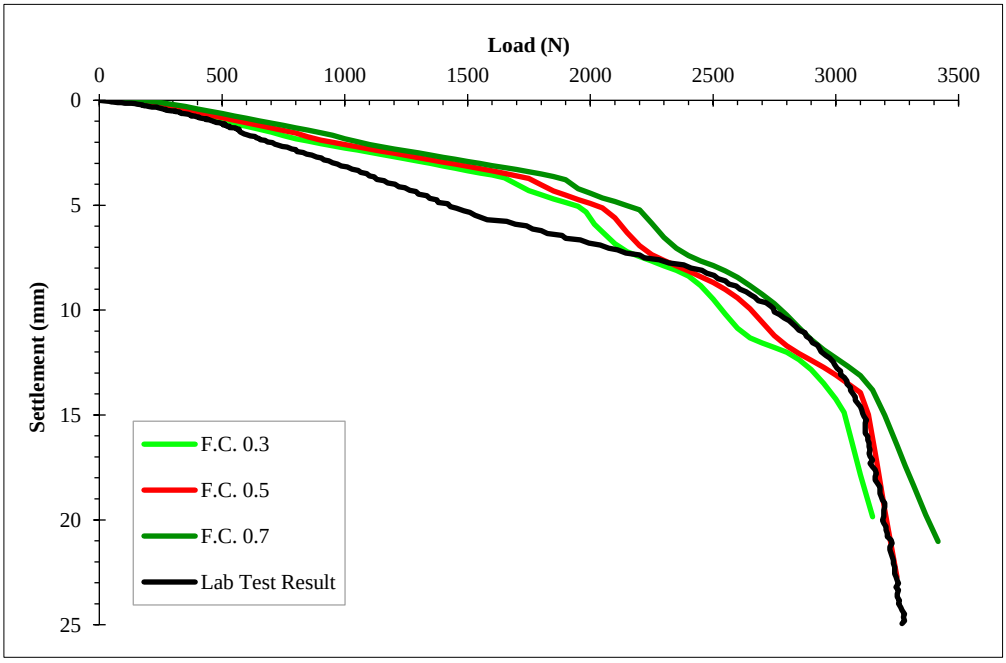

Figure 10. Load-Settlement Curves for Different Friction Coefficients

6. Conclusions

This study aimed to identify influence factors in SSI by analyzing the load-settlement behavior of a pile in sand through a combination of laboratory model tests and FEA. First, a laboratory model test was conducted to measure the behavior of a model pile installed in sand under loading, and the results were used to validate and refine the FEM analysis.

During the analysis process, various parameters, boundary conditions, and contact methods were adjusted to compare and analyze their agreement with the experimental results. The findings indicated that, in sand, selecting an appropriate range of elastic modulus was essential for accurately simulating both the pre-yield linear region and the post-yield plastic region. Additionally, applying a higher friction coefficient (0.5) than the typical literature range (0.3–0.4) resulted in a better match with the experimental data. Furthermore, compared to the general boundary conditions that constrain side boundaries using simple hinge or roller supports, incorporating depth-dependent passive earth pressure provided a more realistic simulation of post-yield behavior. In contact analysis, using only bonded contact led to an overestimation of bearing capacity, as it completely restricted sliding between the pile and soil. However, when frictional contact was applied, the load-settlement curve closely matched the actual laboratory test results, successfully simulating realistic pile behavior.

Through these analyses, it was found that accurately predicting pile bearing capacity and settlement behavior in sand requires a comprehensive approach that considers factors such as the choice of soil material model, parameters (elastic modulus, friction coefficient), the inclusion of passive earth pressure, and the contact method. In particular, the ability to precisely simulate plastic behavior is important for estimating the ultimate load and allowable settlement in pile design. Furthermore, when applying these findings to practical designs, additional factors such as pile surface roughness, soil relative density, and dynamic or cyclic loading conditions in field environments must also be considered. To achieve this, continuous validation and calibration through laboratory model tests or field measurements is essential.

In conclusion, this study integrated lab tests and numerical analysis to specifically illustrate how various factors, such as boundary conditions and contact methods, can influence structure-soil interaction analysis in sand, which are often overlooked. These findings are meaningful as they provide a foundation for ensuring both safety and cost-effectiveness in pile design and construction, while also enhancing the accuracy of predicting complex soil behavior in practical design.

Future research should expand the scope of SSI analysis by considering sand with different relative densities and internal friction angles, clay-sand mixed ground, and dynamic loading conditions. Developing a more comprehensive and versatile SSI modeling approach would be a valuable direction for further study.

7. Declarations

7.1. Author Contributions

Conceptualization, J.G.H. and J.K.; methodology, D.B.L. and J.K.; software, J.K.; validation, J.G.H. and J.Y.L.; formal analysis, J.K.; investigation, D.B.L. and J.K.; resources, J.G.H. and J.K.; data curation, J.Y.L. and J.K.; writing—original draft preparation, J.K.; writing—review and editing, J.G.H. and J.Y.L., visualization, J.K.; supervision, J.G.H.; project administration, J.G.H. All authors have read and agreed to the published version of the manuscript.

7.2. Data Availability Statement

The data presented in this study are available on request from the corresponding author.

7.3. Funding and Acknowledgments

This research was supported by the Chung-Ang University Graduate Research Scholarship in 2021. This research was supported by the MSIT (Ministry of Science and ICT), Korea, under the ITRC (Information Technology Research Center) support program (IITP-2024-2020-0-01655) supervised by the IITP (Institute of Information & Communications Technology Planning & Evaluation). This work was also supported by Korea Planning & Evaluation Institute of Industrial Technology funded by the Ministry of the Interior and Safety (MOIS, Korea). [Project Name: Development of Advanced Technology for National Seismic Hazard Map and Design Standard Using Quaternary Fault Information / Project Number: RS-2025-02653118].

7.4. Conflicts of Interest

The authors declare no conflict of interest.

8. References

[1] Carbonari, S., Dezi, F., & Leoni, G. (2011). Linear soil-structure interaction of coupled wall-frame structures on pile foundations. Soil Dynamics and Earthquake Engineering, 31(9), 1296–1309. doi:10.1016/j.soildyn.2011.05.008.

[2] Rha, C., & Taciroglu, E. (2007). Coupled Macroelement Model of Soil-Structure Interaction in Deep Foundations. Journal of Engineering Mechanics, 133(12), 1326–1340. doi:10.1061/(asce)0733-9399(2007)133:12(1326).

[3] Markou, G., AlHamaydeh, M., & Saadi, D. (2018). Effects of the soil-structure-interaction phenomenon on RC structures with pile foundations. 9th GRACM International Congress on Computational Mechanics, 4-6 June, 2018, Chania, Greece.

[4] Hokmabadi, A. S., Fatahi, B., & Samali, B. (2014). Assessment of soil-pile-structure interaction influencing seismic response of mid-rise buildings sitting on floating pile foundations. Computers and Geotechnics, 55, 172–186. doi:10.1016/j.compgeo.2013.08.011.

[5] Ritter, M. G., Menegotto, M. L., Costella, M. F., Pavan, R. C., & Pilz, S. E. (2020). Analysis of soil-structure interaction in buildings with deep foundation. Revista IBRACON de Estruturas e Materiais, 13(2), 248–273. doi:10.1590/S1983-41952020000200005.

[6] Visuvasam, J., & Chandrasekaran, S. S. (2019). Effect of soil–pile–structure interaction on seismic behaviour of RC building frames. Innovative Infrastructure Solutions, 4(1), 1–9. doi:10.1007/s41062-019-0233-0.

[7] Davisson, M. T. (1970). Design pile capacity. Proceedings of the Conference on Design and Installation of Pile Foundations and Cellular Structures, 13-15 April 1970, Bethlehem, Palestine.

[8] Davisson, M. T. (1972). High capacity piles. Proceedings of Lecture Series on Innovations in. Foundation Construction, 22 March, 1972, Innovations in Foundation Construction, ASCE, Illinois Section, Chicago, United States.

[9] Ghalib, Z. H., & Mahmood, M. R. (2024). The Behavior of Enlarged Base Pile Under Compression and Uplift Loading in Partially Saturated Sand. Civil Engineering Journal (Iran), 10(10), 3240–3252. doi:10.28991/CEJ-2024-010-10-08.

[10] Vesic, A. S. (1977). Design of pile foundations. NCHRP Synthesis of Highway Practice, (42), 1-68.

[11] Perau, E. W. (1997). Bearing capacity of shallow foundations. Soils and foundations, 37(4), 77-83. doi:10.3208/sandf.37.4_77.

[12] Chin, F. K. (1970). Estimation of the ultimate load of piles from tests not carried to failure. 2nd Southeast Asian Conference on Soil Engineering, 11-15 June, 1970, Singapore.

[13] Wang, D., Bienen, B., Nazem, M., Tian, Y., Zheng, J., Pucker, T., & Randolph, M. F. (2015). Large deformation finite element analyses in geotechnical engineering. Computers and Geotechnics, 65, 104–114. doi:10.1016/j.compgeo.2014.12.005.

[14] Cheng, Y. M., Wong, H., Leo, C. J., & Lau, C. K. (2016). Stability of Geotechnical Structures: Theoretical and Numerical Analysis. Frontiers in Civil Engineering: Volume 1. Bentham Science Publishers, Sharjah, United Arab Emirates. doi:10.2174/9781681083032116010l.

[15] Potts, D. M. (2003). Numerical analysis: a virtual dream or practical reality? Géotechnique, 53(6), 535–573. doi:10.1680/geot.53.6.535.37330.

[16] Bakroon, M., Aubram, D., & Rackwitz, F. (2017). Geotechnical large deformation numerical analysis using implicit and explicit integration. 3rd International Conference on New Advances in Civil Engineering, 28-29 April, 2017, Helsinki, Finland.

[17] Wei, W., Zhao, Q., Jiang, Q., & Grasselli, G. (2018). Three new boundary conditions for the seismic response analysis of geomechanics problems using the numerical manifold method. International Journal of Rock Mechanics and Mining Sciences, 105, 110–122. doi:10.1016/j.ijrmms.2018.03.009.

[18] Zdravković, L., & Potts, D. M. (2010). Application of Numerical Analysis in Geotechnical Engineering Practice. GeoFlorida, 69–88. doi:10.1061/41095(365)4.

[19] Cividini, A., Gioda, G., & Sterpi, D. (2019). On the influence of strain softening in the numerical analysis of geotechnical problems. Geoecology and Computers, 207–213. doi:10.1201/9780203753620-30.

[20] Karpurapu, G. R., & Bathurst, R. J. (1988). Comparative analysis of some geomechanics problems using finite and infinite element methods. Computers and Geotechnics, 5(4), 269–284. doi:10.1016/0266-352X(88)90007-9.

[21] Qiu, G., Henke, S., & Grabe, J. (2009, May). Applications of Coupled Eulerian-Lagrangian method to geotechnical problems with large deformations. 2009 SIMULIA Customer Conference, 18-21 May 2009, London, United Kingdom.

[22] Tang, L., Cong, S., Xing, W., Ling, X., Geng, L., Nie, Z., & Gan, F. (2018). Finite element analysis of lateral earth pressure on sheet pile walls. Engineering Geology, 244, 146–158. doi:10.1016/j.enggeo.2018.07.030.

[23] Wang, Z. H., & Zhou, J. (2011). Three-dimensional numerical simulation and earth pressure analysis on double-row piles with consideration of spatial effects. Journal of Zhejiang University: Science A, 12(10), 758–770. doi:10.1631/jzus.A1100067.

[24] Jawad, S., & Han, J. (2021). Numerical Analysis of Laterally Loaded Single Free-Headed Piles within Mechanically Stabilized Earth Walls. International Journal of Geomechanics, 21(5). doi:10.1061/(asce)gm.1943-5622.0001989.

[25] Li, D., Yi, F., Li, X., Chen, S., Hu, Z., & Liu, J. (2024). Excavation Effects on Reinforced Concrete Pile Foundations: A Numerical Analysis. Buildings, 14(4), 995. doi:10.3390/buildings14040995.

[26] Zhan-Fang, H., Bai, X. H., Yin, C., & Liu, Y. Q. (2021). Numerical analysis for the vertical bearing capacity of composite pile foundation system in liquefiable soil under sine wave vibration. PLoS ONE, 16(3), 248502. doi:10.1371/journal.pone.0248502.

[27] Saeedi, M., Dehestani, M., Shooshpasha, I., Ghasemi, G., & Saeedi, B. (2018). Numerical analysis of pile-soil system under seismic liquefaction. Engineering Failure Analysis, 94, 96–108. doi:10.1016/j.engfailanal.2018.07.031.

[28] Ohta, Y., & Nakata, Y. (2025). Micromechanical Behavior of Pipe-Soil Interaction Under Lateral Loading of Buried Pipe Using 3D Dem. IOP Conference Series: Earth and Environmental Science, 1480(1), 12105. doi:10.1088/1755-1315/1480/1/012105.

[29] Elsiragy, M., Azzam, W., & Kassem, E. M. (2025). Experimental and Numerical Study of Enlarged-Head Monopile Under Lateral Load in Soft Clay. Civil Engineering Journal (Iran), 11(2), 453–471. doi:10.28991/CEJ-2025-011-02-04.

[30] Chauhan, V. B., & Dasaka, S. M. (2022). Active earth pressure on retaining wall with a relief shelf: a novel analytical method. Innovative Infrastructure Solutions, 7(1), 99. doi:10.1007/s41062-021-00690-y.

[31] Belytschko, T., & Black, T. (1999). Elastic crack growth in finite elements with minimal remeshing. International journal for numerical methods in engineering, 45(5), 601-620. doi:10.1002/(SICI)1097-0207(19990620)45:5<601::AID-NME598>3.0.CO;2-S.

[32] Smith, D. A. (2012). Well-posed two-point initial-boundary value problems with arbitrary boundary conditions. Mathematical Proceedings of the Cambridge Philosophical Society, 152(3), 473–496. doi:10.1017/S030500411100082X.

[33] Schweiger, H. F. (2008). The Role of Advanced Constitutive Models in Geotechnical Engineering. Geomechanics and Tunnelling, 1(5), 336–344. doi:10.1002/geot.200800033.

[34] Cui, Y., & Zhang, G. (2012). The elasticity-plasticity analysis of composite foundation with lime-soil pile by FEM. Applied Mechanics and Materials, 170–173, 762–765. doi:10.4028/www.scientific.net/AMM.170-173.762.

[35] Potts, D. M., Zdravković, L., Addenbrooke, T. I., Higgins, K. G., & Kovačević, N. (2001). Finite element analysis in geotechnical engineering: application, Thomas Telford, London, United Kingdom. doi:10.1680/feaigea.27831.

[36] Owen, D. R. J., & Hintou, E. (1981). Finite elements in plasticity: Theory and practice. Applied Ocean Research, 3(3), 149. doi:10.1016/0141-1187(81)90117-6.

[37] Al-Soudani, W.H.S., & Albusoda, B.S. (2021). Evaluating End-Bearing and Skin-Friction Resistance of Test Pipe Pile in Sand Soil. Modern Applications of Geotechnical Engineering and Construction. Lecture Notes in Civil Engineering, Vol 112. Springer, Singapore. doi:10.1007/978-981-15-9399-4_3.

[38] Kuwajima, K., Hyodo, M., & Hyde, A. F. (2009). Pile Bearing Capacity Factors and Soil Crushabiity. Journal of Geotechnical and Geoenvironmental Engineering, 135(7), 901–913. doi:10.1061/(asce)gt.1943-5606.0000057.

[39] Ismael, N. F. (1989). Skin Friction Of Driven Piles In Calcareous Sands. Journal of Geotechnical Engineering, 115(1), 135–139. doi:10.1061/(ASCE)0733-9410(1989)115:1(135).

[40] Yuan, M., & Poulos, H. G. (1987). Effect of loading rate on pile skin friction in sands. International Journal of Rock Mechanics and Mining Sciences & Geomechanics Abstracts, 24(3), 114. doi:10.1016/0148-9062(87)90762-5.

[41] Tiwari, B., & Al-Adhadh, A. R. (2014). Influence of Relative Density on Static Soil-Structure Frictional Resistance of Dry and Saturated Sand. Geotechnical and Geological Engineering, 32(2), 411–427. doi:10.1007/s10706-013-9723-6.

[42] Prekop, L. (2017). Modelling the pile load test. MATEC Web of Conferences, 107, 00033. doi:10.1051/matecconf/201710700033.

[43] Prekop, L. (2017). Modeling the load test of vertical resistance of pile. Key Engineering Materials, 738, 310–318. doi:10.4028/www.scientific.net/KEM.738.310.

[44] Xu, C., & Li, Y. (2014). A simulation study of bearing capacity of bored piles in Jinghe bridge based on ANSYS. Applied Mechanics and Materials, 556–562, 704–707. doi:10.4028/www.scientific.net/AMM.556-562.704.

[45] Zhao, M. H., Liu, D. P., Zhang, L., & Jiang, C. (2008). 3D finite element analysis on pile-soil interaction of passive pile group. Journal of Central South University of Technology (English Edition), 15(1), 75–80. doi:10.1007/s11771-008-0016-9.

[46] Tra, H. T., Huynh, Q. T., & Keawsawasvong, S. (2024). Estimating the Ultimate Load Bearing Capacity Implementing Extrapolation Method of Load-Settlement Relationship and 3D-Finite Element Analysis. Transportation Infrastructure Geotechnology, 11(4), 2764–2789. doi:10.1007/s40515-023-00332-z.

[47] Das, B. M. (1994). Principles of Geotechnical Engineering. PWS Publishing Company, Boston, United States.

[48] Wang, Y., Xiong, F., & Ren, J. (2022). Numerical Simulation and Application of Zero-Thickness Contact Surface Element with Variable Shear Stiffness on Pile Foundation. Advances in Civil Engineering, 7343847. doi:10.1155/2022/7343847.

[49] Ninić, J., Stascheit, J., & Meschke, G. (2014). Beam-solid contact formulation for finite element analysis of pile-soil interaction with arbitrary discretization. International Journal for Numerical and Analytical Methods in Geomechanics, 38(14), 1453–1476. doi:10.1002/nag.2262.